



Green synthesis and characterizations of TiO₂ nanoparticles using *Cordia myxa* and *Ziziphus spina* extracts

Raghad A. Rasheed, Maysoun F. A. Alias*

Department of Physics, College of Science, University of Baghdad, Baghdad, Iraq

*) Email: maysoun.ahmed@sc.uobaghdad.edu.iq

Received 11/9/2025, Received in revised form 23/11/2025, Accepted 25/11/2025, Published 15/1/2026

The environmentally friendly synthesis process is used to produce titanium dioxide nanoparticles (TiO₂ NPs) using *Cordia myxa* (TiO₂-C) and *Ziziphus spina* (TiO₂-Z) extracts. TiO₂ nanoparticle properties are studied by various physical examinations such as energy dispersive X-ray spectroscopy (EDX), X-ray diffraction (XRD), field emission scanning electron microscopy (FESEM) and UV-vis spectrophotometer. EDX showed the composition of titanium and oxygen. For the purpose of structural characterizing TiO₂ nanoparticles, XRD confirmed that the TiO₂-C NPs exhibited a rutile phase and a tetragonal structure, although anatase phase for TiO₂-Z, with average crystal sizes of about 12.1636 nm and 8.245 nm respectively. FESEM micrograph of TiO₂-C nanoparticles showed that the particles are agglomerated and uneven, the average diameter of the particles is roughly \approx 42.36 nm, and whereas the FESEM micrograph of TiO₂-Z nanoparticles showed, the particles are primarily smooth-surfaced and polygonal, with average diameter \approx 106.95 nm. UV-vis spectroscopy measurements indicate that TiO₂-C had a 3.15 eV direct energy gap, while for TiO₂-Z it is 3.0 eV.

Keywords: Green synthesis; Nanoparticles; Titanium dioxide.

1. INTRODUCTION

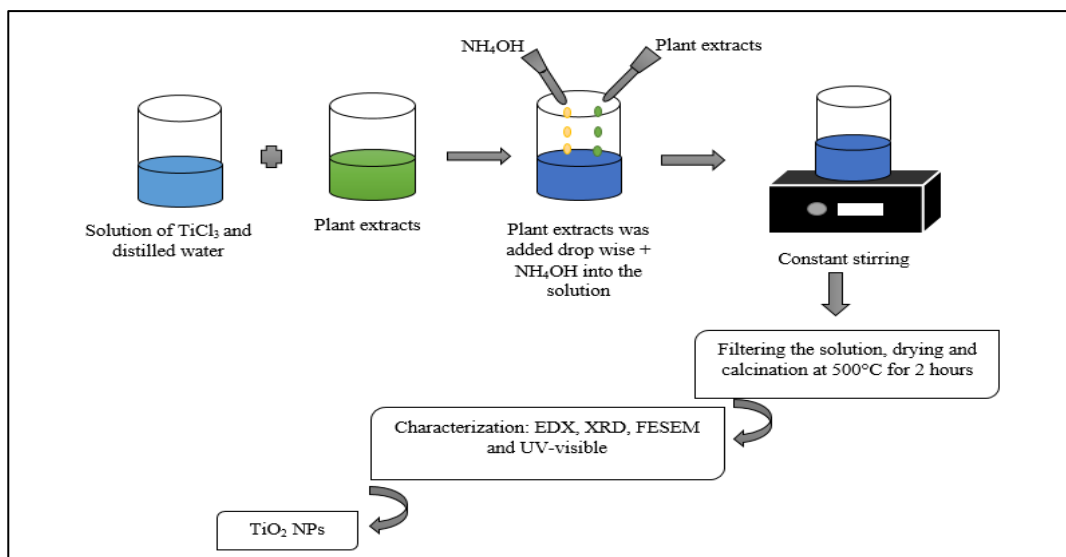
Green technology has garnered significant attention in the last decade. The green technique appears to be a well-liked approach to addressing the regular depletion of natural resources without causing harm to them. The development and applications of nanomaterials in the fields of energy, food, medicine, sensors, and optoelectronics are the main emphasis of this technology. [1] Numerous physical and chemical methods can be used to produce metal nanoparticles (NPs) and metal oxide nanostructures, including lithography, electrospinning, and sputtering. However, they can be somewhat expensive, and handling dangerous substances can be harmful to one's health. In this sense, no hazardous chemicals,

high-pressure reactors, or high temperatures are needed when using the green synthesis method. Above all, it produces biodegradable waste with a lower chance of contamination in the end [2,3]. In recent years, scientists have become interested in green chemistry, which uses environmentally safe substances like plants, fruits, flowers, algae, yeasts, bacteria, and fungi to create nanoparticles [4–9]. Materials known as nanostructured semiconductor metal oxides are important to the creation of the majority of electronic instruments, including sensors, diodes, transistors, and solar cells, [10-14] for several metal oxides, in the scientific community, TiO₂ nanoparticles are of a great deal of interest [15]. In addition to its corrosion resistance, titanium dioxide also has favorable chemical and physical properties, making it an appealing substance for use in solar cell applications. [16-18]. TiO₂ is also used like gas sensor [19,20], a biological sensor, and in medical diagnostics [21,22]. Titanium has three standard crystal structure types: anatase, rutile and brookite [23]. In comparison to rutile and brookite, anatase has the greatest photocatalytic and antibacterial activity. Even though anatase is kinetically stable, at higher temperatures it turns rutile. It is shown that rutile is thermodynamically stable at room temperature [24]. This group consists of anatase and rutile phases that are tetragonal in shape, whereas the brookite phase is orthorhombic in shape [22,25]. This research paper aims to prepare and characterize TiO₂ nanoparticles using *cordia myxa* and *ziziphus spina* extracts by the green method and investigation their composition, structure morphology and optical properties.

2. EXPERIMENTAL

2.1 Synthesis of plant extracts and TiO₂ NPs

The plant leaves of *Cordia myxa* and *Ziziphus spina* are collected from University of Baghdad's College of Science's garden and they are picked from the tree and cleaned three or four times with distilled water and running water, each one is cleaned separately to remove dust and dirt before being allowed to dry. Titanium (III) chloride (TiCl₃) and (NH₄OH) ammonium hydroxide is purchased from the Alpha Chemika India company, and deionized water (DW) is used. With an electric grinder, *cordia myxa* and *ziziphus spina* leaves are ground, and in plastic containers they stored their powder. A regulated amount of distilled deionized water (1:10) is added to the plant powder, i.e. 10 ml of water per 1 gram of plant, and stirred vigorously for 30 min at 70°C. Whatman filter No.1 paper is used to filter out the extracts, and the filtrate is then kept in a refrigerator at 4°C. Each extract is prepared separately. Titanium dioxide has been prepared by green synthesis method by adding 13ml of TiCl₃ is added to 100 ml DW, then adding 25 ml of plant extracts once for *cordia myxa* and another for *ziziphus spina*, followed by (NH₄OH) of 98% purity, and agitating the mixture on a magnetic stirrer at 70-80°C for 1h. The sediment is centrifuged for 15 minutes at 4,000 rpm. Several washings are done with DW to achieve a pH of 7 [26]. The resulting mixture was then put into a crucible and heated to 500 °C for two hours, to produce TiO₂ with *cordia myxa* TiO₂-C and TiO₂ with *ziziphus spina* TiO₂-Z [27]. The objective of the study is to examine the biosynthesis of TiO₂ nanoparticles using aqueous extracts of *Cordia myxa* and *Ziziphus spina* plant leaves as a reducing and stabilizing agent, as well as the impact of this process on the structure and properties of the final nanoparticles [28,29]. Figures 1 illustrates all these processes.



Figures 1 TiO₂ nanoparticle synthesis diagram.

Energy dispersive X-ray spectroscopy (EDX) is used to determine the composition of the samples. X-ray diffraction techniques are used to describe the crystallite size and structure of prepared TiO₂ nanoparticles. The morphological characteristics of the prepared nanoparticles are identified using field emission scanning electron microscope (FESEM) and optical characteristics are examined using UV-Vis spectroscopy.

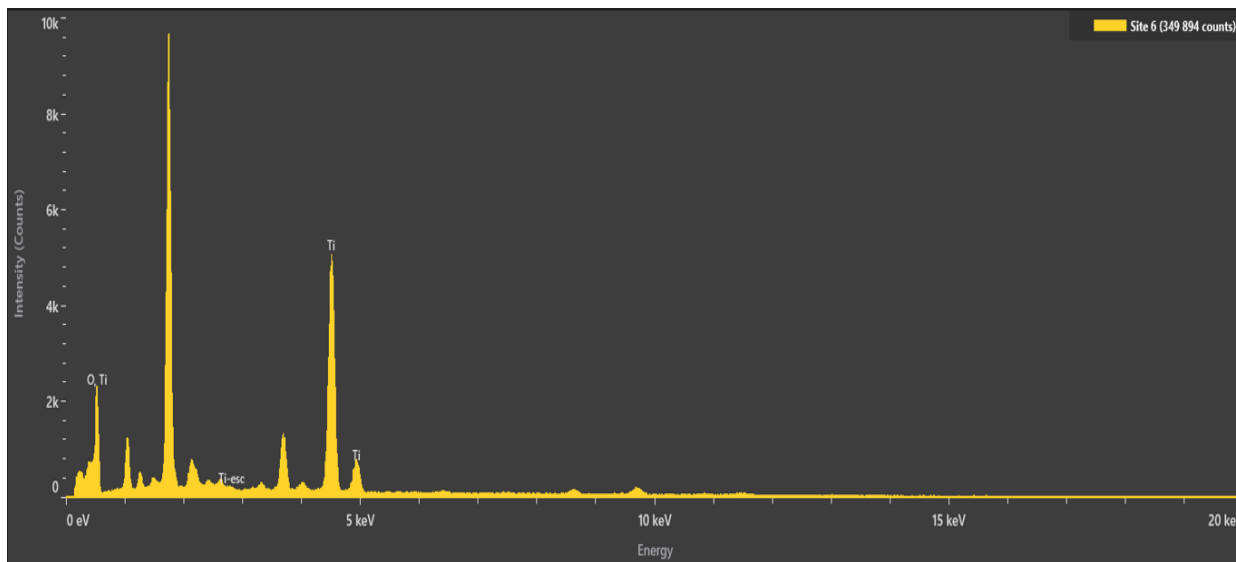
3. RESULTS AND DISCUSSION

3.1 Compositional analysis

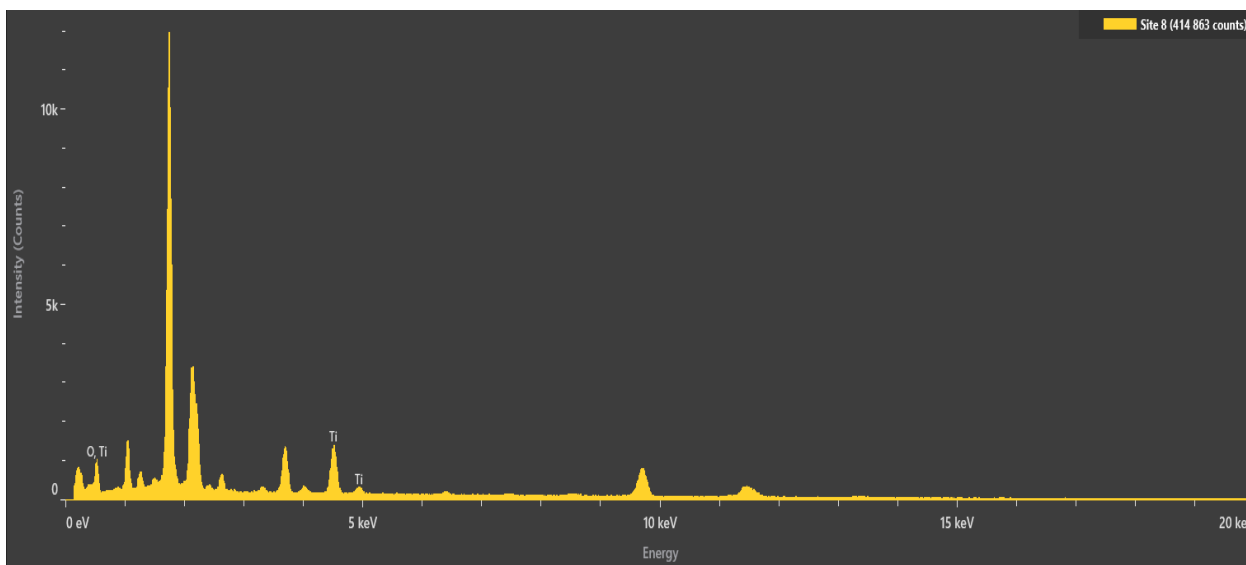
3.1.1 Energy dispersive X-ray spectroscopy (EDX)

The elemental composition of nanomaterials is ascertained by energy dispersive X-ray spectroscopy technique of SEM, provides information on the percentage of the materials that each element occupies, using Axia ChemiSEM (Thermo scientific) at ALKHORA COMPANY SEM LAB-BAGHDAD-IRAQ INSPECT F 50 FE-SEM. Figures 2a and 2b display the sample's EDX compositional mapping for TiO₂-C and TiO₂-Z, respectively. TiO₂ nanoparticles made from *Ziziphus spina-christi* extract verify that titanium (Ti) and oxygen (O) are the primary constituents. Ti and O are discovered to have atomic percentages of 21.5% and 78.5%, respectively, and weight percentages of 45.0% and 55.0%. These numbers demonstrate the successful production of the oxide and are in accordance with the stoichiometry of TiO₂ (Ti:O = 1:2). The absence of other peaks indicating other elements suggests that the sample is highly pure. These results are agreement with other researchers [30].

As for TiO₂-Z prepared by the green method using *Ziziphus spina* extract, verified that titanium and oxygen are the primary constituents. Ti and O are discovered to have atomic percentages of 13.4% and 86.6%, respectively, and weight percentages of 31.7% and 68.3%. The sample shows oxygen and titanium peaks. The percentages of the elements in the TiO₂ sample are produced by green synthesis.



(a)



(b)

Figure 2 (a) EDX for TiO₂-C, (b) EDX for TiO₂-Z.

3.2 Structural properties

3.2.1 X-ray diffraction (XRD)

In Figures 3a, an X-ray diffraction pattern can be seen of titanium dioxide powder that prepared using *cordia myxa* extract TiO₂-C powder, in contrast Figures 3b illustrates X-ray diffraction of titanium dioxide that prepared using *ziziphus spina* extract TiO₂-Z powder using (Benchtop XRD) diffractometer (Cu-K α radiation, $\lambda=1.5418 \text{ \AA}$), (company: Malvern panalytical) at ALKHORA COMPANY SEM LAB-BAGHDAD-IRAQ INSPECT F 50 FE-SEM. For all samples prepared for TiO₂-C, the patterns indicated polycrystalline with tetragonal structure and rutile phase [31]. Table 1 gives the values of structural and geometric parameters. Figures 3a shows peaks for (TiO₂-C) NPs at $2\theta = 27.465^\circ, 36.097^\circ, 39.232^\circ, 41.265^\circ, 44.091^\circ, 54.366^\circ, 56.689^\circ, 62.775^\circ, 64.121^\circ, 65.572^\circ$ and 69.072° corresponding to

(110), (101), (200), (111), (210), (211), (220), (002), (310), (221) and (301) planes respectively. Matching the data with the JCPDS card: (96-410-2356) [32].

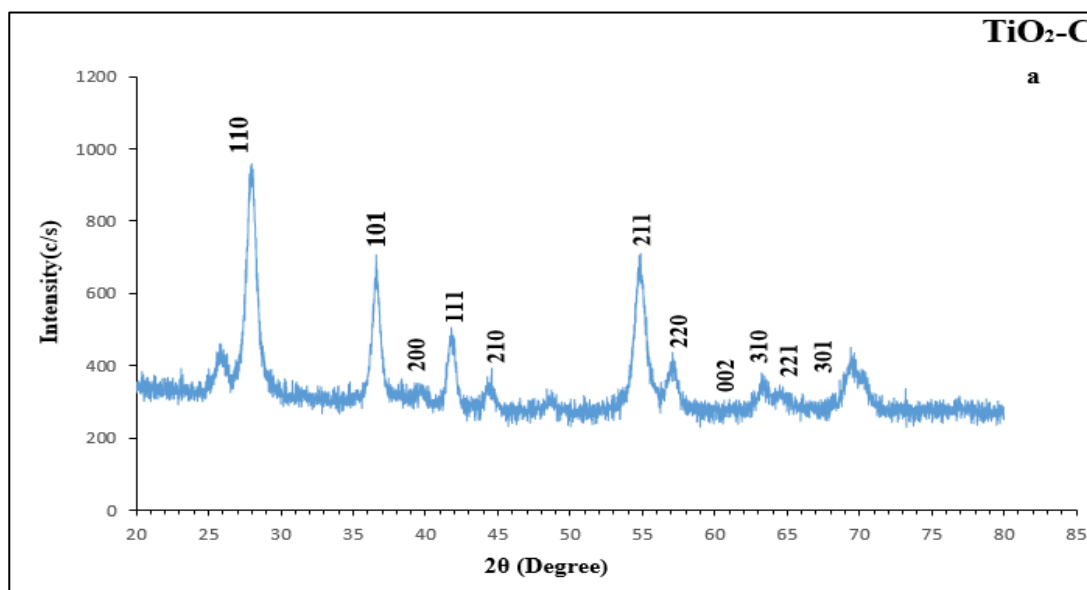
Figures 3b and Table 2 display the TiO₂-Z NPs' XRD pattern, the patterns indicated polycrystalline with tetragonal structure and anatas phase [31], the TiO₂-Z NPs has peaks at 2θ= 25.7872°, 27.9393°, 36.5531°, 38.3122°, 41.7114°, 48.5158°, 54.7845°, 56.6776°, 63.1612°, 69.7507° and 75.7918° corresponding to (101), (103), (004), (112), (200), (202), (105), (211), (213), (204) and (116) plans respectively, Matching the data with the JCPDS card: (96-152-6932) [33]. In Table 1, TiO₂-C NP and TiO₂-Z NPs crystallite sizes are provided. By applying Bragg's law, d_{hkl} is calculated [34]:

$$n \lambda = 2 d_{hkl} \sin \theta \tag{1}$$

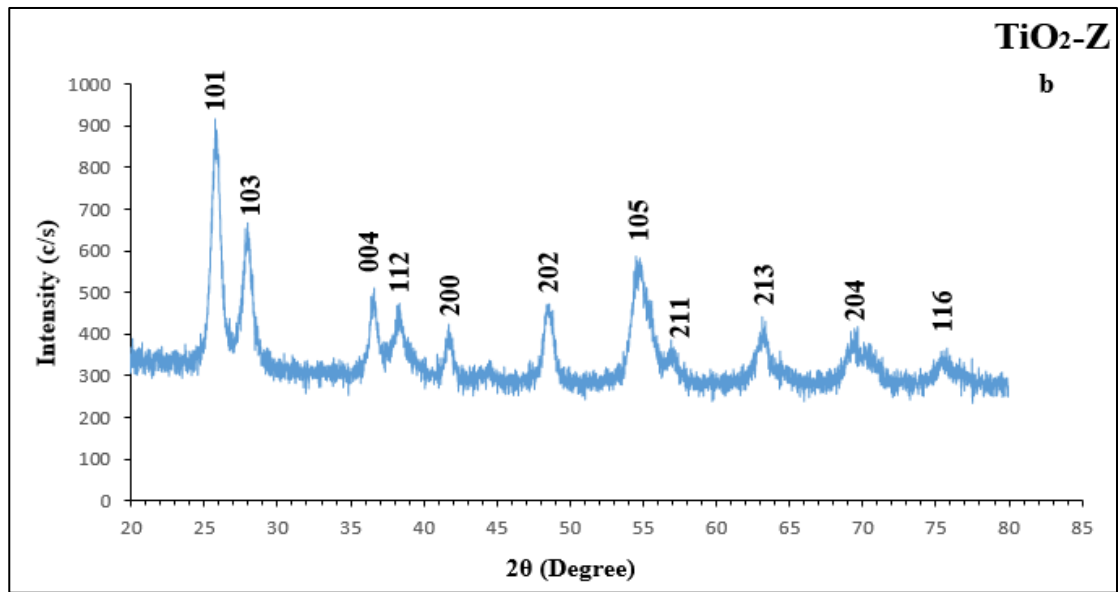
In contrast, by using the Scherrer equation, the value C.S is determined [35]:

$$C.S = K \lambda \beta \cos \theta \tag{2}$$

where C.S is crystallite size, K is constant Scherrer (0.9), λ is the monochromatic wavelength of X-ray (0.154061 nm), θ is the Bragg diffraction angle, and β is full width at half maximum (FWHM). Typical average crystalline sizes of TiO₂-Z and TiO₂-C are 8.245 nm and 12.163 nm, respectively.



(a)



(b)

Figures 3 (a) XRD pattern for TiO₂-C-NPs powder, (b) XRD pattern for TiO₂-Z-NPs powder.

Table 1 The structural parameters TiO₂-C-NPs.

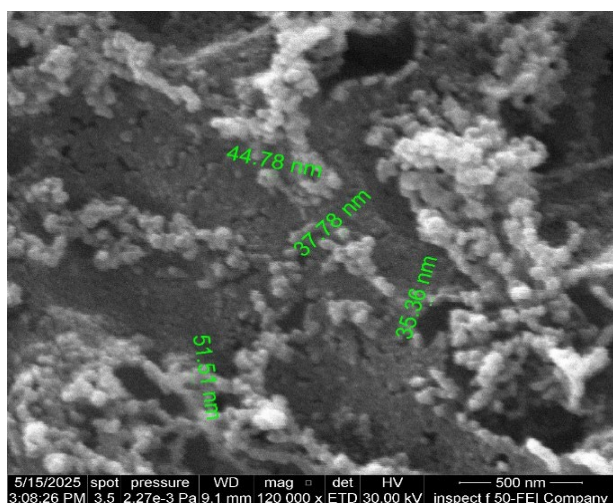
TiO ₂ -C-NPs					
2θ (Deg.)	FWHM(Deg.)	d _{exp} (Å°)	C.S(nm)	d _{hkl} (Å°)	phase
27.465	0.8643	3.44975	8.2	110	Rutile - tetragonal
36.097	0.8077	3.19071	8.0	101	
39.232	0.6425	2.45588	10.4	200	
41.265	1.7047	2.27922	2.9	111	
44.091	0.6511	2.16109	14.1	210	
54.366	0.7004	2.03885	13.2	211	
56.689	0.1324	1.87248	49.1	220	
62.775	0.9271	1.67391	8.4	002	
64.121	0.8092	1.61398	10.3	310	
65.572	1.215	1.45869	4.3	221	
69.072	1.6643	1.34963	4.9	301	

Table 2 The structural parameters of TiO₂-Z-NPs.

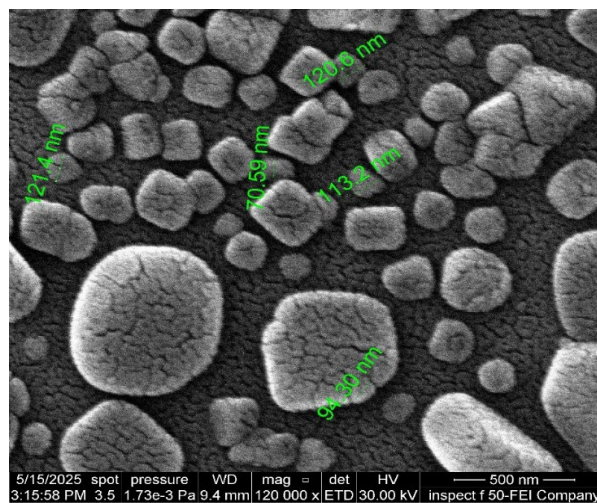
TiO ₂ -Z-NPs					
2θ (Deg.)	FWHM(Deg.)	d _{exp} (Å°)	C.S(nm)	d _{hkl} (Å°)	phase
25.7872	0.7255	3.45207	9.6	101	anatas-tetragonal
27.9393	0.798	3.19086	8.0	103	
36.5531	0.5819	2.45628	11.8	004	
38.3122	0.8156	2.34745	5.9	112	
41.7114	0.5665	2.16367	15.6	200	
48.5158	0.8115	1.87492	11.6	202	
54.7845	1.3761	1.67427	7.0	105	
56.6776	1.6784	1.62276	5.8	211	
63.1612	0.928	1.47089	7.9	213	
69.7507	2.1458	1.34716	4.4	204	
75.7918	2.4909	1.25409	3.1	116	

3.2.2 Field emission scanning electron microscopy (FESEM)

The FESEM micrograph of TiO₂-C nanoparticles made using *Cordia myxa* extract showed agglomerated and uneven particles using 120,000 magnifications [36], using Inspect™ F50 (company: FEI, Thermo Fisher Scientific) at ALKHORA COMPANY SEM LAB-BAGHDAD-IRAQ INSPECT F 50 FE-SEM. The average diameter of the particles is roughly 42.36 nm [37], while their sizes varied from 35.36 to 51.51 nm. The phytochemicals in the extract may have worked as both stabilizing and reducing agents, which is why the aggregation is seen. The synthesized nanoparticles are verified to be in the rutile phase by XRD examination, which correlates with the observed morphology. The relatively larger particle size and aggregated structure are consistent with the denser and more thermodynamically stable nature of the rutile phase, as shown in the Figures 4a. According to a FESEM examination, the TiO₂ nanoparticles made from *Ziziphus spina-christi* extract are primarily smooth-surfaced and polygonal, with (average ≈ 106.95 nm) and a range of 70.59 to 121.4 nm. XRD verified the anatase phase, which usually showed smaller crystallite sizes, however the comparatively large particle sizes shown here could be explained by grain development and particle aggregation during calcination, which are controlled by phytochemicals in the plant extract [38], according to the Figures 4b.



Figures 4a FESEM image for TiO₂-C



Figures 4b FESEM image for TiO₂-Z

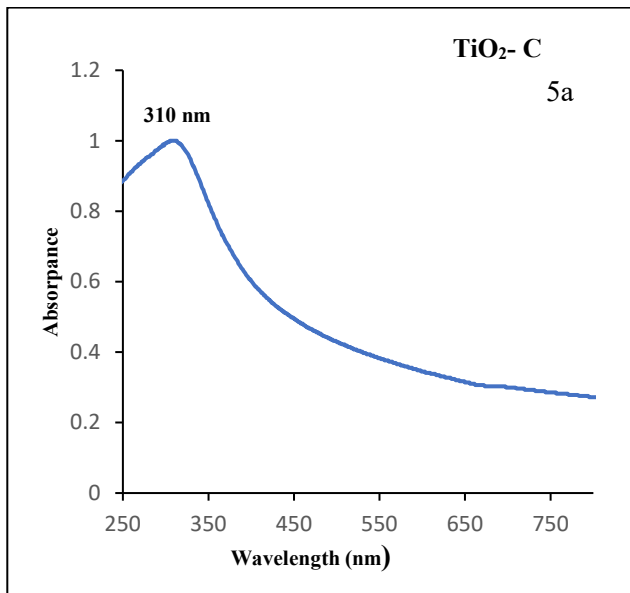
3.3 Optical properties

Using two plant extracts, the green-synthesized TiO₂ NPs' UV-vis spectra are captured one for *cordia myxa* TiO₂-C and another from *ziziphus spina* TiO₂-Z by. The optical study included absorbance spectrum and optical energy gap for powders produced by green synthesis are evaluated using Optima SP-3000 UV-Vis spectrophotometer (supplied by Optima Company) covering a range from (200-1200) nm at ALKHORA COMPANY SEM LAB-BAGHDAD-IRAQ INSPECT F 50 FE-SEM. Figs 5 a and 6 a revealed the absorbance spectra for both prepared TiO₂ NPs samples in the wavelength rang 300–800 nm. The presence of the TiO₂ NPs is confirmed by the absorbance peaks, which are between 300 and 400 nm (310 nm for TiO₂-C and 307 nm for TiO₂-Z). These results are agreement with other researchers [39].

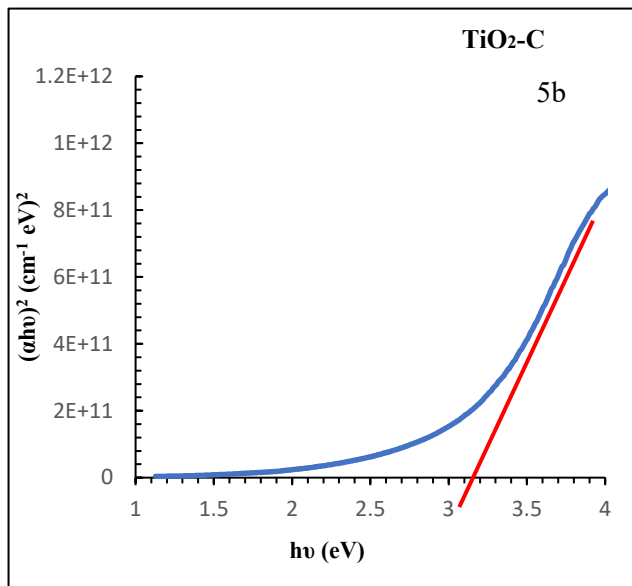
By applying the Tauc relationship, the band-gap energy calculated. The absorption coefficient and incident photon energy (hv) determine the optical band gap (E_g) in the manner described by the following relationship.

$$\alpha hv = A (hv - E_g)^n \quad (3)$$

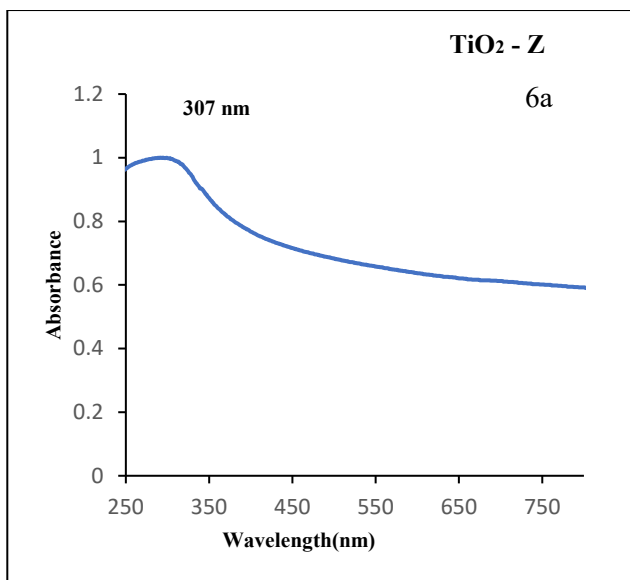
where A is the optical constant, α is the absorption coefficient, h is the Planck's constant, ν is the frequency of the incident photon and n is the number characterizing the nature of the transition process (here n = 1/2 for allowed direct transition and n = 2 for allowed indirect transition) [40]. E_g is obtained by making a plot $(\alpha hv)^2$ versus hv as shown in the Figs 5b and 6b, which represents the allowed direct optical energy gap of TiO₂-C is equal to 3.15eV and the energy gap for (TiO₂-Z) is equal to 3.0 eV respectively. These values are in line to results of another researchers [27,41].



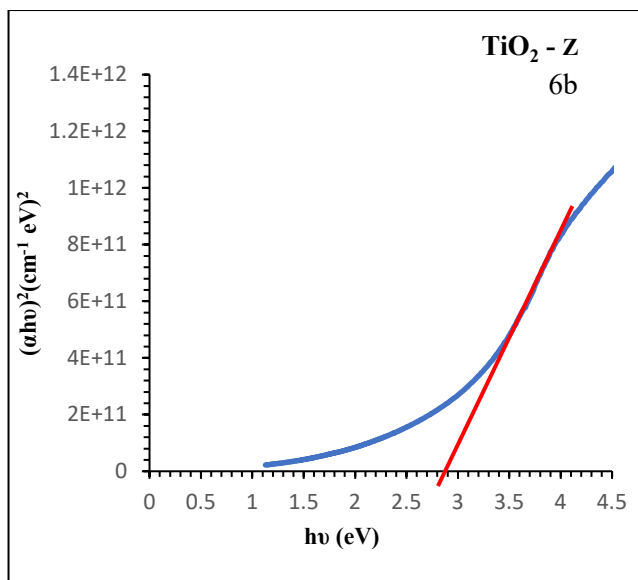
Figures 5a Absorbance vs. wavelength of TiO₂-C



Figures 5b Variation of $(\alpha h\nu)^2$ vs $h\nu$ of TiO₂-C.



Figures 6a Absorbance vs. wavelength of TiO₂-Z



Figures 6b Variation of $(\alpha h\nu)^2$ vs $h\nu$ of TiO₂-Z.

4. CONCLUSIONS

Titanium dioxide nanoparticles were synthesized successfully using an environmental, low-cost, safe and simple method from *cordia myxa* and *ziziphus spina* extract with TiCl₃ aqueous solution. The diagnostic techniques EDX, XRD, FESEM and UV-Vis were utilized to describe the composition, structure, morphology and optical of the produced particles. The physical examinations of prepared TiO₂-C and TiO₂-Z reveal that the nanoparticle structures were different in shape and size, due to differences in the chemical composition of both plant extracts. The prepared TiO₂ had direct energy gap. Our results clearly indicate that TiO₂-C and TiO₂-Z could effectively use for engineering and medical applications.

References

- [1] J. Singh, T. Dutta, K.-H. Kim, M. Rawat, P. Samddar, P. Kumar, J. Nanobiotechnol. 16 (2018) 1 [10.1186/s12951-018-0408-4](https://doi.org/10.1186/s12951-018-0408-4)
- [2] Maksood Adil Mahmoud Al-Doori, Nahedh Ayad Faris, Noor Adnan Mahmood, Asaad T. Al-Douri, Luay Mannaa ibrahim, Amna M. Al-Tikrity, Exp. Theo. NANOTECHNOLOGY 9 (2025) 555 <https://doi.org/10.56053/9.4.555>
- [3] S. Jain, M.S. Mehata, Sci. Rep. 7 (2017) 1 <https://doi.org/10.1038/s41598-017-15724-8>
- [4] K.M. Kumar, B.K. Mandal, K.S. Kumar, P.S. Reddy, B. Sreedhar, Spectrochim. Acta A 102 (2013) 128 [10.1016/j.saa.2012.10.015](https://doi.org/10.1016/j.saa.2012.10.015)
- [5] C. Liu, Q. Kuang, Z. Xie, L. Zheng, CrystEngComm 17 (2015) 6308 <https://doi.org/10.1039/C5CE01162K>
- [6] C.P. Devatha, A.K. Thalla, Synth. Inorg. Nanomater. (2018) 169 [10.1016/B978-0-08-101975-7.00007-5](https://doi.org/10.1016/B978-0-08-101975-7.00007-5)
- [7] Nabaa Abbas Zubaidi, Mustafa Kareem AL-Azzawi, Marwan Saleh Mahdi, Murtadha Hadi Ajmi, Experimental and Theoretical NANOTECHNOLOGY 9 (2025) 15 <https://doi.org/10.56053/9.S.15>
- [8] G. Benelli, Synth. Inorg. Nanomater. 9 (2019) 1275 <https://doi.org/10.3390/nano9091275>
- [9] Y.L. Pang, S. Lim, H.C. Ong, W.T. Chong, Appl. Catal. A 481 (2014) 127 <https://doi.org/10.1016/j.matpr.2018.08.058>
- [10] Y. Wu, Q. Huang, J. Nie, J. Liang, N. Joshi, T. Hayasaka, S. Zhao, M. Zhang, X. Wang, L. Lin, J. Nanosci. Nanotechnol. 19 (2019) 5310 <https://doi.org/10.1166/jnn.2019.16859>
- [11] N. Joshi, F.M. Shimizu, I.T. Awan, J.C. M'Peko, V.R. Mastelaro, O.N. Oliveira, L.F. Da Silva, IEEE Sens. (2016) 1 <https://doi.org/10.3390/mi11060624>
- [12] Y. Wu, N. Joshi, S. Zhao, H. Long, L. Zhou, G. Ma, B. Peng, O.N. Oliveira, A. Zettl, L. Lin, Appl. Surf. Sci. 529 (2020) 147110 [10.20944/preprints202111.0334.v1](https://doi.org/10.20944/preprints202111.0334.v1)
- [13] N. Joshi, T. Hayasaka, Y. Liu, H. Liu, O.N. Oliveira, L. Lin, Microchim. Acta 185 (2018) 213 <https://doi.org/10.1016/B978-0-12-820727-7.00004-5>
- [14] A. Gaiardo, B. Fabbri, A. Giberti, V. Guidi, P. Bellutti, C. Malagù, M. Valt, G. Pepponi, S. Gherardi, G. Zonta, A. Martucci, M. Sturaro, N. Landini, Sens. Actuators B 237 (2016) 1085 <https://doi.org/10.3390/proceedings1040398>
- [15] R.A. Gonçalves, R.P. Toledo, N. Joshi, O.M. Berengue, Molecules 26 (2021) 2236 <https://doi.org/10.3390/molecules26082236>
- [16] I.O. Selyanin, A.S. Steparuk, R.A. Irgashev, A.V. Mekhaev, G.L. Rusinov, A.S. Vorokh, Chim. Techno Acta 7 (2020) 140 [10.15826/chimtech.2020.7.4.01](https://doi.org/10.15826/chimtech.2020.7.4.01)
- [17] Asaad T. Al-Douri, Alaa A. Khaleel, Luay Mannaa ibrahim, Abeer Talib Abdulqader, Ammr Khalid Shihab, Mustafa Khaleel Ibrahim, Maksood Adil Mahmoud Al-Doori, Exp. Theo. NANOTECHNOLOGY 9 (2025) 563 <https://doi.org/10.56053/9.4.563>
- [18] M.M. Abbas, M. Rasheed, Iraqi J. Phys. 19 (2021) 1 [10.30723/ijp.19.48.1-9](https://doi.org/10.30723/ijp.19.48.1-9)
- [19] S. Srivastava, S. Kumar, V.N. Singh, M. Singh, Y.K. Vijay, Int. J. Hydrogen Energy 36 (2011) 6343 <https://doi.org/10.1002/PSSA.201329289>
- [20] Hayder Subhi Faisal, Cezar Mohamed Ahmed, Ayaa Ayad abeed, Mais Qasem Mohammed, Asaad T. Al-Douri, Semaa Amer Ghanam, Zeena T. Khattab, Aya Abdullateef Ezat, Maksood Adil Mahmoud Al-Doori, Nida Muhsin Ali, Mohammed Ameri, Mohammad Mutlag Salih, Exp. Theo. NANOTECHNOLOGY 9 (2025) 571 <https://doi.org/10.56053/9.4.571>
- [21] S.M. Hunagund, V.R. Desai, D.A. Barretto, M.S. Pujar, J.S. Kadadevarmath, S. Vootla, A.H. Sidarai, J. Photochem. Photobiol. A 346 (2017) 159 [10.1016/j.jre.2019.09.006](https://doi.org/10.1016/j.jre.2019.09.006)
- [22] H. Ennaceri, M. Boujnah, A. Taleb, A. Khaldoun, R. Sáez-Araoz, A. Ennaoui, A. Benyoussef, Int. J. Hydrogen Energy 42 (2017) 19467 <https://doi.org/10.3390/met13071163>
- [23] N.S. Allen, N. Mahdjoub, V. Vishnyakov, P.J. Kelly, R.J. Kriek, Polym. Degrad. Stab. 150 (2018) 31 <https://doi.org/10.1016/j.polymdegradstab.2018.02.008>

- [24] M. Pawar, S. Topcu Sengođdular, P. Gouma, J. Nanomater. (2018) 5953609 <https://doi.org/10.1155/2018/5953609>
- [25] M.J. AlSultani, M.F.A. Alias, Iraqi J. Sci. 66 (2025) 2336 <https://doi.org/10.24996/ijs.2025.66.6.12>
- [26] M.J. Tuama, M.F.A. Alias, Karbala Int. J. Mod. Sci. 9 (2023) 11 [10.1007/s43994-025-00243-4](https://doi.org/10.1007/s43994-025-00243-4)
- [27] G. Nabi, W. Raza, M.B. Tahir, J. Inorg. Organomet. Polym. Mater. 30 (2020) 1425 [10.1007/s10904-019-01248-3](https://doi.org/10.1007/s10904-019-01248-3)
- [28] B. Ankamwar, U.K. Sur, M. Salgaonkar, L.S. Sarma, Adv. Sci. Eng. Med. 8 (2016) 868 [10.1088/2632-959X/ab844c](https://doi.org/10.1088/2632-959X/ab844c)
- [29] T.B. Alobaidi, A.I. Alwared, J. Ecol. Eng. 23 (2021) 315 <https://doi.org/10.12911/22998993/143971>
- [30] A.S. Alhazmi, T. Elshebiny, A. Alayyash, S.N. Asiri, F. Alharbi, Open Dent. J. 18 (2024) 1 [10.2174/0118742106347125241101100417](https://doi.org/10.2174/0118742106347125241101100417)
- [31] R. Tariq, D.E. Al-Mammar, Ibn Al-Haitham J. Pure Appl. Sci. 36 (2023) 221 <https://doi.org/10.30526/36.4.3161>
- [32] E. Dorolti, L. Cario, B. Corraze, E. Janod, C. Vaju, H.J. Koo, M.H. Whangbo, J. Am. Chem. Soc. 132 (2010) 5704 <https://doi.org/10.1021/cm001099b>
- [33] T.E. Weirich, M. Winterer, S. Seifried, H. Hahn, H. Fuess, Ultramicroscopy 81 (2000) 263 [10.1016/s0304-3991\(99\)00189-8](https://doi.org/10.1016/s0304-3991(99)00189-8)
- [34] H.H. Kadhim, K.A. Saleh, Iraqi J. Sci. 63 (2022) 1894 [doi: 10.24996/ijs.2022.63.5.4](https://doi.org/10.24996/ijs.2022.63.5.4)
- [35] T.M. Al-Saadi, Ibn Al-Haitham J. Pure Appl. Sci. 35 (2022) 94 <https://doi.org/10.30526/35.4.2872>
- [36] A. Ghareeb, A. Fouda, R.M. Kishk, W.M. El Kazzaz, Microb. Cell Fact. 23 (2024) 341 [10.21203/rs.3.rs-8173031/v1](https://doi.org/10.21203/rs.3.rs-8173031/v1)
- [37] M. Aravind, M. Amalanathan, M.S. Mary, SN Appl. Sci. 3 (2021) 409 [10.1007/s42452-021-04281-5](https://doi.org/10.1007/s42452-021-04281-5)
- [38] Alaa M. Theban, Falah H. Ali, Experimental and Theoretical NANOTECHNOLOGY 9 (2025) 51 <https://doi.org/10.56053/9.S.51>
- [39] Zainab R.Muslim, Ali Q . Kadhum, Zina A. Al Shadidi, Smah A.Kadhum, Experimental and Theoretical NANOTECHNOLOGY 9 (2025) 79 <https://doi.org/10.56053/9.S.79>
- [40] Björn Reetz, Andreas Frehn, Wolfgang Budweiser, William Bishop, Exp. Theo. NANOTECHNOLOGY 9 (2025) 465 <https://doi.org/10.56053/9.3.465>
- [41] D. Asmat-Campos, M.L. Rojas, A. Carreño-Ortega, Cleaner Eng. Technol. 17 (2023) 100702 [10.1016/j.clet.2023.100702](https://doi.org/10.1016/j.clet.2023.100702)